We are IntechOpen,
the world's leading publisher of
Open Access books
Built by scientists, for scientists

6,900
Open access books available

185,000
International authors and editors

200M
Downloads

154
Countries delivered to

Our authors are among the

TOP 1%
most cited scientists

12.2%
Contributors from top 500 universities

CLARIVATE ANALYTICS

BOOK CITATION INDEX

INDEXED

WEB OF SCIENCE™

Selection of our books indexed in the Book Citation Index
in Web of Science™ Core Collection (BKCI)

Interested in publishing with us?
Contact book.department@intechopen.com

Numbers displayed above are based on latest data collected.
For more information visit www.intechopen.com

Synthesis Processes for Li-Ion Battery Electrodes – From Solid State Reaction to Solvothermal Self-Assembly Methods

Verónica Palomares[1] and Teófilo Rojo[1,2]
[1]Universidad del País Vasco/Euskal Herriko Unibertsitatea,
[2]CIC Energigune,
Spain

1. Introduction

Since 1990, Li-ion batteries became essential for our daily life, and the scope of their applications is currently expanding from mobile electronic devices to electric vehicles, power tools and stationary power grid storage. The ever-enlarging market of portable electronic products and the new demands of the transportation market and stationary storage require cells with enhanced energy density, power density, cyclability and safety. In short, to get better performance. These new needs have boosted research and optimization of new materials for Li-ion batteries.
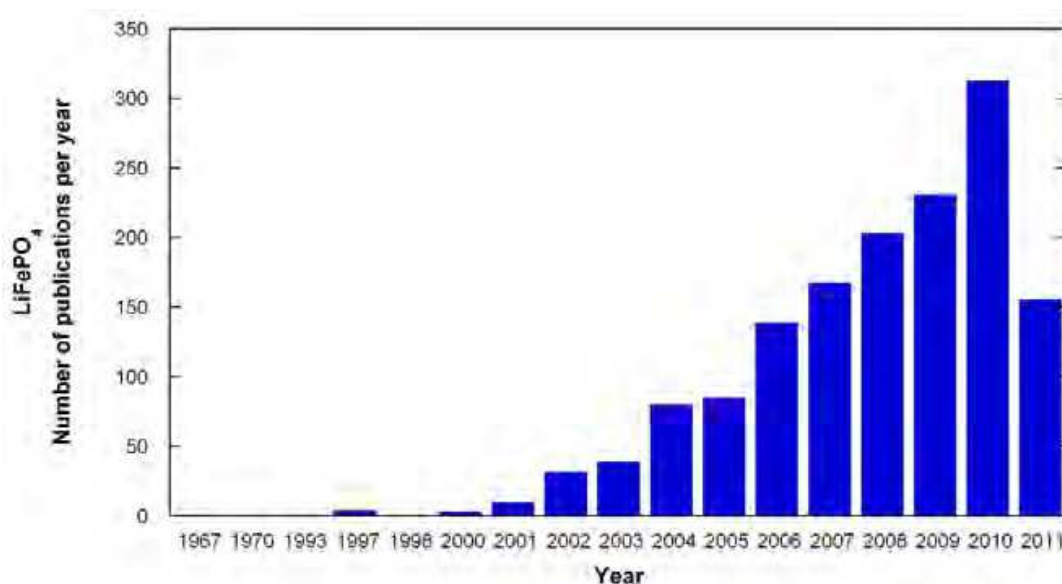

Fig. 1. Number of scientific publications about $LiFePO_4$ material in the last 40 years. Source: Scifinder Scholar™ 2007.

The aim of this work is to show the evolution of chemical preparative methods used to synthesize new electroactive materials or to ameliorate electrochemical performance of the existing ones, and to compare the improvement of performance achieved by the new

materials processing. This way, the synthesis methods of several electrodic materials for Li-ion batteries will be analyzed. Mainly cathode materials, such as layered oxides derived from $LiCoO_2$ or $LiMn_2O_4$ spinel derivatives will be described. Olivine $LiFePO_4$ phase, a material that, besides having the right voltage to present safety attributes is made of low cost and abundant elements, will be specially remarked because of its extraordinary importance in the last years (figure 1).

In recent years, nanoscience has irrupted strongly in the battery materials field. Not only the performance of previously known materials was improved significantly by nanodispersion and nanostructuring, but also new materials and electrochemical reactions have emerged. Thus, the fabrication of nanostructured electrodes has become one of the main goals in battery materials.

First, the small size and large surface area of nanomaterials provide greater contact area between the electrode material and the electrolyte. Second, the distance the Li ions have to diffuse across the electrode is shortened. Therefore, faster charge/discharge ability, that is, a higher rate capability, can be expected for nanostructured electrodes. For very small particles, the chemical potentials for lithium ions and electrons may be modified, resulting in a change of electrode potential. Moreover, the range of composition over which solid solutions exist is often more extensive for nanoparticles, and the strain associated with intercalation is often better accommodated. Furthermore, even new electrochemical reactions, such as conversion reactions for anodes have appeared in nanostructured electrodes. Thus, morphology and size of electrode materials have become a key factor for their performance and the synthesis processes have been evolved toward nanoarchitectured materials.

This chapter will provide an overview on most used synthesis methods from the beginning of Li-ion batteries major research up to the newest ones. Materials performance evolution due to new processing systems will be discussed.

2. Conventional synthesis methods

Classical synthesis methods can be classified in solid reactions and solution methods, according to the precursors used (Figure 2).

Ceramic process is the simplest and most traditional synthesis method because of its easy procedure and easy scale-up. It consists on manual grinding of the reactants and their subsequent heating in air, oxidative, reducing or inert atmosphere, depending on the targeted compound. The great disadvantage of this method is the need for high calcination temperatures, from 700 to 1500º C, which provokes the growth and sinterization of the crystals, leading to micrometer-sized particles (>1 μm) [Eom, J. et al. (2008); Cho, Y. & Cho, J. (2010); Mi, C.H. et al. (2005); Yamada, A. et al. (2001)]. The macroscopic dimensions of as synthesized particles leads to limited kinetics of Li insertion/extraction and makes difficult the proper carbon coating of phosphate particles [Song, H-K. et al. (2010)]. For this reason it was necessary to add carbon during or after the grinding process, which implies the use of an extra grinding step [Liao, X.Z. et al. (2005); Zhang, S.S. et al. (2005); Nakamura, T. et al. (2006); Mi, C.H. et al. (2005)]. Mechanochemical activation can be considered as a variant of the ceramic method, but the final calcination temperature is lower, of about 600º C [Kwon, S.J. et al. (2004); Kim, C.W. et al. (2005); Kim, J-K. et al. (2007)]. This way, grain size is slightly lower due to mechanical milling.
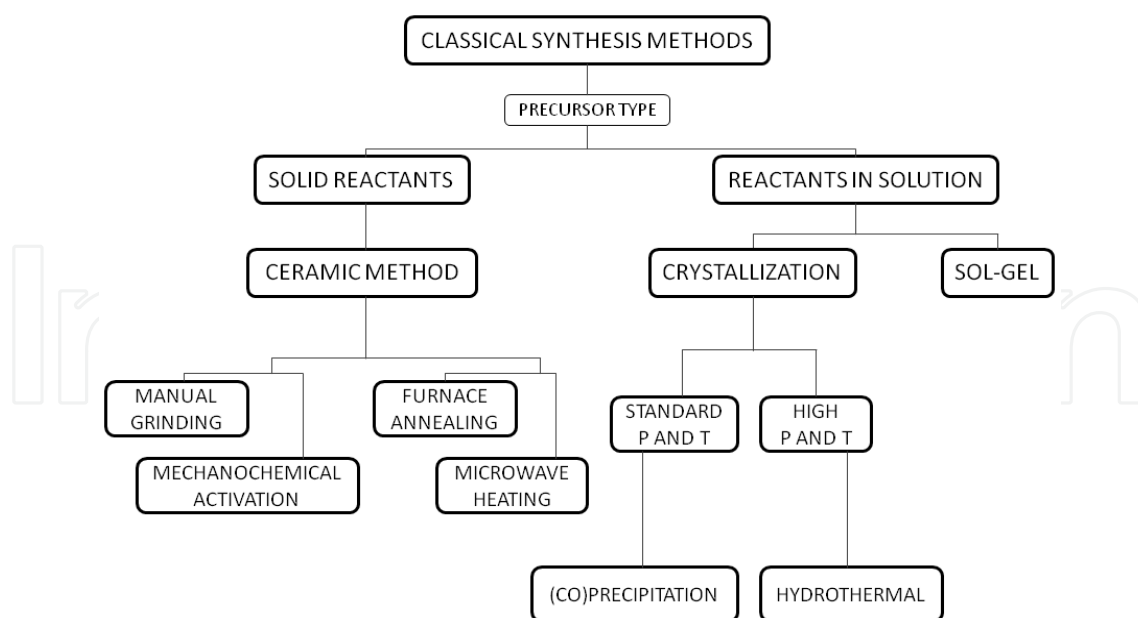
Fig. 2. Schematic of the classical synthesis methods used to prepare electrode materials for Li-ion batteries.

Hand-milled precursors can also be activated by microwave radiation [Song, M-S. et al. (2007)]. If at least one of the reactants is microwave sensitive, the mixture can get sufficiently high temperatures so as to achieve the reaction and obtain the targeted compound in very short heating times, between 2 and 20 minutes. This factor makes this synthesis method an economic way to obtain desired phases. Sometimes, when a carbonaceous composite is desired, active carbon can be used to absorb microwave radiation and to heat the sample [Park, K.S. et al. (2003)]. Organic additives such as sucrose [Li, W. et al. (2007)], glucose [Beninati, S. et al. (2008)] or citric acid [Wang, L. et al. (2007)] can be used in the initial mixture in order to get in situ carbon formation. Oxide-type impurity generation is not usually indicated in literature, but, sometimes, the reaction atmosphere is so reducing that iron carbide (Fe_7C_3) or iron phosphide (Fe_2P) are generated as secondary phases [Song, M-S. et al (2008)]. Particle size of phosphates obtained by this synthesis method ranges between 1 and 2 μm, but two effects have been reported with regard to this parameter. The growth of particles was correlated with the increase of microwave exposure times. However, in the presence of greater amounts of carbon precursor the particles decrese in size leading to 10-20 nm particles.

Synthesis methods that comprise the dissolution of all reactants promote greater homogeneity in final samples. Both coprecipitation and hydrothermal processes consist on the precipitation and crystallization of the targeted compound under normal (coprecipitation) or high (hydrothermal) temperature and pressure conditions. Usually coprecipitation involves a subsequent heating process, which enhances particle growth [Park, K.S. et al. (2004); Yang, M-R. et al. (2005)]. Nevertheless, recent advances in direct precipitation method have produced narrow particle size materials, of about 140 nm, with enhanced electrochemical properties in terms of specific capacity (147 mAh g^{-1} at 5C rate) as well as in terms of cyclability (no significant capacity fade after more than 400 cycles) with no carbon coating [Delacourt, C. et al. (2006)]. On the other hand, hydrothermal synthesis is an effective method to obtain well-crystallized materials with well-defined morphologies, where no additional high-temperature treatment is needed, but no small size particles can

be obtained. Tryphilite crystals of about 1x3 μm have been produced by this method without carbonaceous coating [Yang, S. et al. (2001); Tajimi, S. et al. (2004); Dokko, K. et al. (2007); Kanamura, K. and Koizumi, S. (2008)]. Conductive carbon coating can be produced by using diverse additives that also act as reductive agents, such as sucrose, ascorbic acid [Jin, B. and Gu, H-B. (2008)] or carbon nanotubes [Chen, J. and Whittingham, M.S. (2006)]. The preparation of LiFePO₄ samples by hydrothermal method using heating temperatures below 190° C has been demonstrated to create olivine phases with some inversion between Fe and Li sites, with 7% of the iron atoms in lithium sites, and also the presence of small amounts of Fe(III) in the material. Lithium ion diffusion in LiFePO₄ is one-dimensional, because the tunnels where Li ions are located run along the b axis are not connected, so lithium ions residing in the channels cannot readily jump from one tunnel to another if Fe(III) ions are present. Thus, any blockage in the tunnel will block the movement of the lithium ions. This way, the presence of iron atoms on the lithium sites prevents the diffusion of Li ions down the channels in the structure and jeopardizes electrochemical performance. For this reason, materials synthesized under hydrothermal conditions at 120° C did not reach 100 mAh·g^{-1} [Yang, S. et al. (2001)]. The use of higher temperatures, the addition of L-ascorbic acid, carbon nanotubes or a subsequent annealing process (500-700° C) under nitrogen atmosphere can produce ordered LiFePO₄ phases that are able to deliver sustainable capacities of 145 mAh·g^{-1} [Whittingham, M.S. et al. (2005); Chen, J. et al. (2007)].

A study by Nazar et al. on the different variables that influence the hydrothermal processes concludes that, in the first place, crystal size can be controlled by reaction temperature and precursors concentration inside the reactor, because higher precursor concentration creates higher quantity of nucleation sites, thus leading to smaller particle sizes. In the second place, decrease of synthesis temperature also entails smaller particle size, but shorter reaction times do not have remarkable influence on the product morphology, once the minimum reaction time is surpassed [Ellis, B. et al. (2007a)].

Among the solution methods, sol-gel process is a classical method used to obtain different types of inorganic materials [Kim, D.H. and Kim, J. (2007); Pechini, P. Patent; Baythoun, M.S.G. and Sale, F.R. (1982)]. Apart from the homogeneity promoted by the starting reactants solution, this method allows the introduction of a carbon source that can act as particle size control factor, leaves a carbon that can be useful to create carbon composites, and, finally, allows the use of lower heating temperatures than in solid state reaction methods [Hsu, K-F. et al. (2004); Chung, H-T. et al. (2004); Choi, D. and Kumta, P.N. (2007)]. This way, synthesizing one phase by ceramic or sol-gel method under the same thermal treatments allows getting lower particle size for sol-gel samples [Piana, M. et al. (2004)].

3. New synthetic methods directed towards nanostructured materials

Apart from the classical preparative methods, a wide variety of synthetic approaches has been developed to improve the rate capabilities of the materials. The rate determining step in the electrodes of Li-ion batteries is supposed to be solid state diffusion. Faster kinetics is expected with smaller particle size because the diffusion length is shorter. For this purpose, Li-ion battery electrode materials have been built in very different nanoarchitectures, such as nanotubes, nanobelts, nanowires, nanospheres, nanoflowers and, nanoparticles. These synthesis methods have been focused to obtaining nanostructured electrode materials (figure 3).
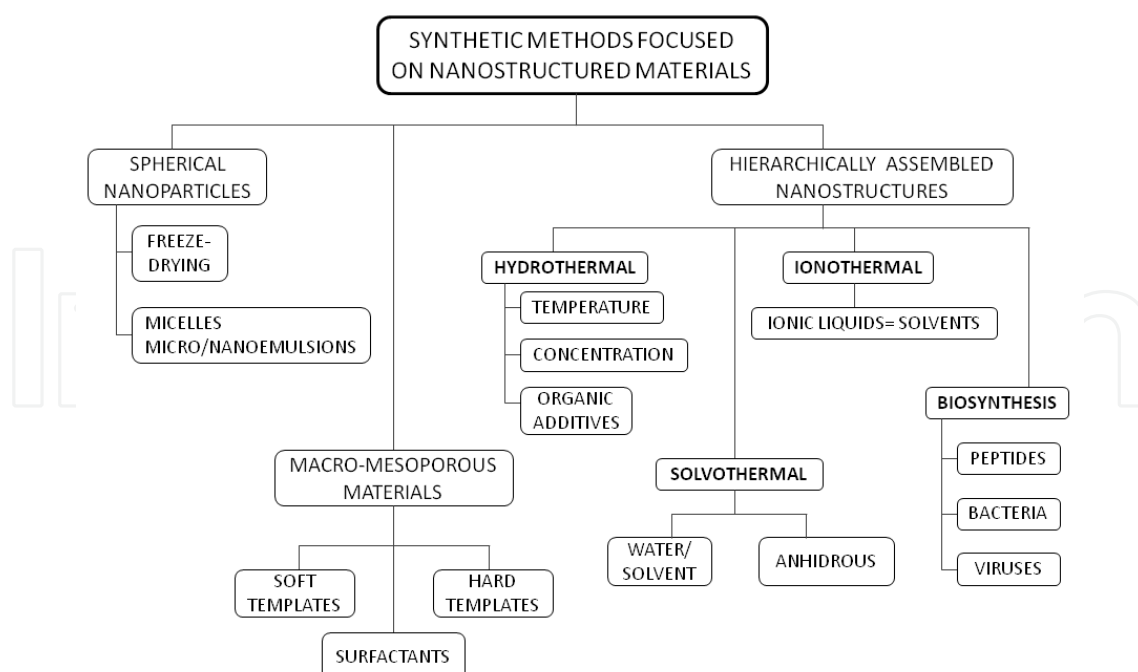
Fig. 3. Schematic of the synthesis methods used to prepare nanostructured electrode materials for Li-ion batteries.

3.1 Synthesis of spherical nanoparticles

Freeze-drying synthesis method presents advantages such as homogeneity of reactants, the possibility of introducing a carbon source and the use of lower calcinations temperatures [Palomares, V. et al. (2009a)]. Rojo et al. applied this synthesis process to prepare LiFePO$_4$/C composites for the first time, getting nanosized phosphate particles of 40 nm completely surrounded by a carbonaceous web with 141 mAh·g^{-1} specific capacity at 1C rate [Palomares, V. et al. (2007)].

Freeze-drying process consists on solvent elimination from a frozen solution by sublimation. Sublimation process is thermodynamically favoured versus fusion or evaporation below solvent triple point pressure and temperature conditions (figure 4). First, the reactant solution needs to be frozen (from A to B point), and under low temperature, and low pressure conditions a direct sublimation process can be feasible (from C to E points).

However, the presence of any solute does alter triple point location. Freeze-drying technique allows maintaining stoichiometry and homogeneity of a multicomponent solution in the final dried product [Paulus, M. (1980)], and also provides promotes small size particles.

The starting solution is frozen so millimeter sized droplets with high specific area are formed. These droplets are dried under low temperature and vacuum conditions in order to get a spongy solid that is calcined at low temperature to obtain the targeted compound. Optimization of this synthesis method has led to 10 nm sized LiFePO$_4$ particles embedded in a carbonaceous web that enhances the electrochemical performance due to greater surface area of nanosized particles and to homogeneous carbon coating that connects the active material [Palomares et al, (2011)].
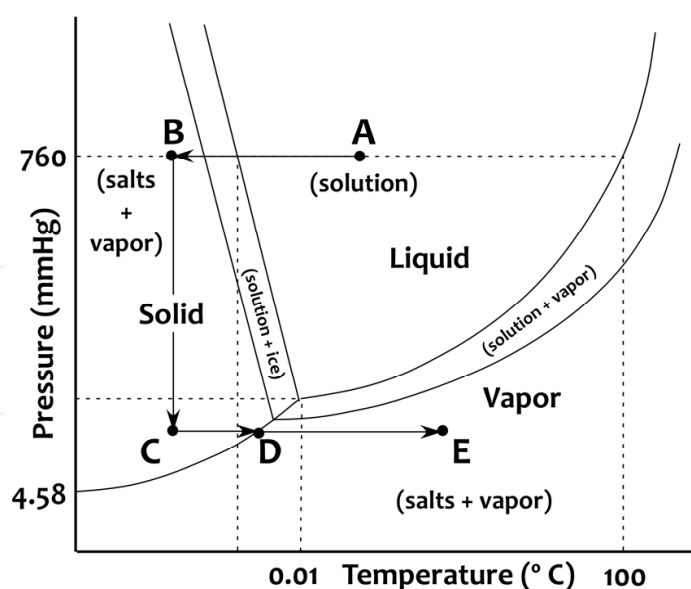
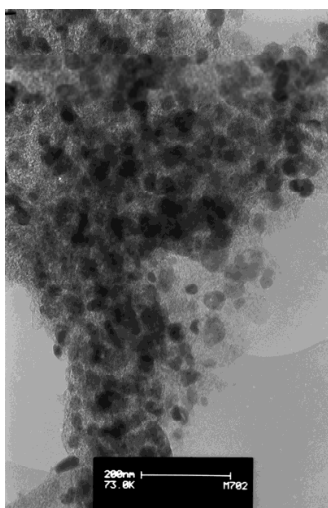Fig. 4. Water phase diagram. Freeze-drying process is marked by arrows.

Fig. 5. LiFePO$_4$/C nanocomposites prepared by freeze-drying. [Palomares et al.(2007)]

Although carbonaceous coating for these freeze-dried materials is very homogeneous, it has been demonstrated that it can only replace a small proportion of the conductive carbon additives used to prepare positive electrodes based on LiFePO$_4$ compound [Palomares, V. et al. (2009b)]. Deep characterization of *in situ* produced carbon showed that, in spite of its high specific surface, it presents high disorder, which is not favourable to a good electrochemical performance, and does not have enough conductivity to act as conductive additive in these cathodes.

Swollen micelles and microemulsions make up another synthesis method that lead to discrete nanoparticles with controlled chemical composition and size distribution [Li, M. et al. (1999)]. In this synthesis method, chemical reactions are carried out in an aqueous media within a restricted volume, limited by the array of surfactant and co-surfactant molecules. The versatility of this technique allows its use in the preparation of different electrode materials for lithium ion batteries. The obtained solid products exhibit a controlled size and shape, remaining well dispersed due to their isolation from other particles by the surfactant

molecules during the synthesis [Aragón, M.J. et al. (2010)]. There are three different processes to obtain nanoparticles by the reverse micelles methods. The first one consists on mixing different emulsions which contain the necessary reagents in aqueous solution, so coalescence of pairs of droplets results in the formation of the solids in a confined volume. The second one involves reacting by diffusion of one of the reagents through the oil phase and the surfactant molecular layer. The last one requires thermolysis within individual droplets to get the target compound of a controlled size. $LiCoO_2$ cathode material has been prepared by the last process, providing 140 mAh·g^{-1}. Thermal decomposition of the micelles was achieved by putting the emulsion in contact with a hot organic solvent, such as kerosene at 180° C. $LiMn_2O_4$ was also obtained by the same method, leading to 200 nm diameter particles with good electrochemical performance.

Rod-like $LiFePO_4$/C composite cathodes have also been synthesized by reverse micelles method, using kerosene with Tween#80 surfactant as oil phase, and annealing the obtained precursor at 650° C in N_2 atmosphere [Hwang, B-J. et al. (2009)]. Morphology of this composite consisted on rod-like porous aggregates made of tiny primary nanoparticles. This special arrangement of primary particles provided better accommodation of volume changes during cycling, better electrical connection with the current collector and efficient electron transport. Galvanostatic cycling of this composite showed very good results for this rod-like composite, with a specific capacity of 150 and 95 mAh·g^{-1} at C/30 and 5C, respectively.

3.2 Synthesis of macro or mesoporous materials

One approach to new positive electrode materials for high rate applications is to synthesize three dimensionally ordered macroporous or mesoporous solids. Such materials are composed of micrometer-sized particles within which identical ordered pores of diameter 2–50 nm exist with walls of 2-8 nm thickness. Unlike nanoparticles, which can become disconnected one from another as they expand or contract on cycling, mesoporous materials, since they have the same dimensions as the intercalation cathodes in conventional lithium-cells, suffer less from the problem of disconnection. Furthermore, they may be fabricated in the same way as conventional materials, yet the internal porosity permits the electrolyte to flood the particles ensuring a high contact area and hence a facile lithium transfer across the interface, as well as short diffusion distances for Li^+ transport within the walls, where intercalation takes place [Bruce, P.G. (2008a)].

Ordered mesoporous solids can be built with silica structures [Bruce, P.G. et al. (2008b)]. The first example of an ordered mesoporous lithium transition-metal oxide, the low temperature polymorph of $LiCoO_2$, has been synthesized and shown to exhibit superior properties as a cathode compared with the same compound in nanoparticle form. This material showed 40 Å size pores and a wall thickness of 70 Å. Synthesis of this sample comprised the use of KIT-6 silica as a template. Impregnation of the silica in Co precursor solution, subsequent annealing and silica template dissolution produced mesostructured Co_3O_4. This porous oxide reacted with LiOH by solid state reaction to get $LiCoO_2$. The ordered mesoporous material demonstrates superior lithium cycling during continuous intercalation/removal for 50 cycles [Jiao, F. Et al. (2005)].

Mesoporous structures can also be prepared by using soft colloidal crystals as templates. In 1997, Velev first reported the use of colloidal latex spheres, in the range of 150 nm to 1 μm as templates to produce silica macroporous structures [Velev, O.D. et al. (1997)]. A colloidal

crystal consists on an ordered array of colloid particle that is analogous to a standard crystal whose repeating subunits are atoms or molecules [Pieranski, P. (1983)]. They are usually formed from closed-packed spheres such as latex, poly(styrene) (PS), silica or PMMA (poly(methyl methacrylate)) microbeads. After infiltration of the precursors solution into the opal structure, the assembly is usually calcined in air at temperatures between 500 and 700° C. This way, void spaces between particles are filled by the fluid precursors, and these latter are converted into a solid before removal of the template material.

Colloidal crystal templates were first reported as additive to form electrode materials for Li-ion batteries in 2002 [Sakamoto, J.S., Dunn, B. (2002)], and has also been used for the preparation of 3-D ordered macroporous $LiMn_2O_4$ spinel [Tonti, D. et al. (2008)]. Lithium iron phosphate has been successfully templated using colloidal crystal templates of PMMA of 100, 140 and 270 nm diameter spheres to produce porous, open lattice electrode materials, which featured pores in the mesoporous (10-50 nm), meso-macroporous (20-80 nm), and macroporous (50-120 nm) ranges, respectively [Doherty, C.M. et al. (2009)]. The well-stacked PMMA colloidal crystals provided robust scaffolding in which the $LiFePO_4$ precursor solution was infiltrated and then condensed. Once the PMMA spheres were removed through the calcinations process at different annealing temperatures ranging from 320 to 800° C, the $LiFePO_4$ featured an open lattice structure with residual carbon left over from the decomposed colloidal crystal template. Figure 6 shows the crystal colloidal systems used for this research, with well-organized, stacked homogeneous diameter spheres, and also the open porous structures of the template $LiFePO_4$, with a continuous open lattice structure with long-range order.
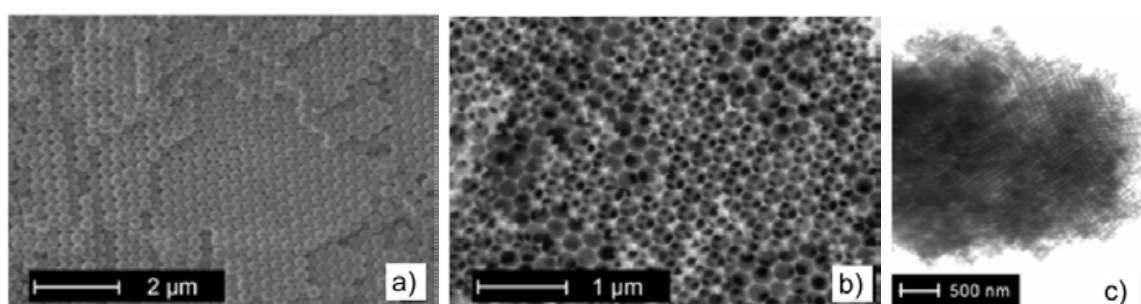

Fig. 6. a) Micrograph of the used colloidal crystal system; b) $LiFePO_4$ templated with 270 nm sized PMMA spheres; and c) Regular channels formed from the closed-packed beads, which allow for good electrolyte access to the $LiFePO_4$ surfaces. (Doherty, C.M. et al. (2009)).

All produced materials suffered from shrinkage of the porous structure, being the pore diameters for each of the samples approximately 40% of the initial bead diameter. Growing crystallite sizes were recorded when the calcination temperature was increased from 500 to 800° C. Despite the higher surface area of the material made from the smallest bead diameter (100 nm), its electrochemical performance was the poorest of the three of them. This can be due to restriction of the electrolyte access caused by poor interconnectivity between the pores that leaves some $LiFePO_4$ surface electrochemically inactive. Micrographs of the sample showed some areas where the small pores had collapsed and become blocked during thermal treatment and, thus, open lattice was not present. For this reason, it can be said that interconnectivity of the pore structure is essential for good electrolyte penetration as well as efficient charge transfer. This way, the templated samples prepared with the larger spheres (270 nm) would offer both good interconnectivity and better electrolyte

access to surfaces within large micrometer-sized $LiFePO_4$ particles. The advantage of using colloidal crystal templating to produce high power $LiFePO_4$ electrodes is that it allows the pore sizes to be tailored while controlling the synthesis conditions. It increases the surface area and decreases the diffusion distance while maintaining an interconnected porous structure to provide efficient charge transfer and reduced impedance.

Mesoporous electrode materials have also been fabricated by using a cationic surfactant in fluoride medium, such as $Li_3Fe_2(PO_4)_3$ [Zhu, S. et al. (2004)]. This material showed an average pore diameter of 3.2 nm and a wall thickness of 2.2 nm. In this case, self-assembly process that leaded to mesoporous material was based on Coulombic interactions between the head groups of the surfactant (cetyltrimethylammonium $CTMA^+$) and F^- ions, that encapsulate Fe^{2+} species. Fe^{2+} ions are located between ion pairs $[LiPO_4Fe^{2+}]$ and $[F^-CTMA^+]$. Cathode performance of this self-assembled $Li_3Fe_2(PO_4)_3$ material was better than the observed in other studies described in literature, with a specific capacity above 100 mAh $\cdot g^{-1}$ at 200 mA $\cdot g^{-1}$.

3.3 Synthesis of nanostructured materials by hydrothermal/solvothermal methods

While the hunt for high performance electrode materials for Li-ion batteries remains the main research objective, cost associated with producing these materials is now becoming another overriding factor. Sustainability, renewability and green chemistry concepts must be also taken into consideration when selecting electrode materials processing methods for the next generation of batteries, especially for high volume applications. Thus, turning to low cost and green systems has led to rediscover hydrothermal and solvothermal approaches for battery materials. Furthermore, solvothermal and hydrothermal processes can be easily tuned to obtain nanostructures using different solvent/cosolvent/surfactant systems.

Obtaining $LiFePO_4$ small sized particles by hydrothermal synthesis method is possible by controlling several factors, as it was proposed in L.F. Nazar's work (2007). In this synthesis method, the main parameters that have influence on particle size in the absence of organic molecules (size modifiers) are reaction temperature and precursor concentration. As is the case for processing methods that require annealing treatments, e.g. sol-gel or ceramic methods, the use of lower temperatures induce the formation of smaller particles. On the other hand, an increase of the reactant concentration creates more nucleation sites and therefore produces much smaller particles. For example, 1-5 µm sized $LiFePO_4$ crystals were obtained by using low concentrations of precursors, but 250 nm size crystals were synthesized when concentration was increased threefold. The effect of both parameters in particle structure and size must be taken into account when trying to produce small sized materials. Although lower reaction temperatures favour smaller particle size, in low temperature hydrothermally synthesized $LiFePO_4$ Fe disorder in the structure was observed, and this structural defect was detrimental to electrochemical performance. Thus, a balance between both parameters must be seeked.

The use of organic compounds in hydrothermal medium can have two effects. First, some specific molecules can control particle morphology, and, second, the organic compounds in the medium serve as reductive agents and carbon precursor in order to get a carbonaceous coating around the particles. When the main purpose of the organic molecule is the attainment of a carbon coating, there exist two possibilities: organic product decomposition

during hydrothermal process, as is the case of ascorbic acid; or the use of a further annealing treatment, as it is necessary for citric acid. Water soluble polymers can also be used as carbon precursors to get nanosized particles. For example, polyacrilic acid leads to 300-500 nm LiFePO$_4$ aggregates made of 75-100 nm size particles. These polymers coordinate strongly to crystal faces, and inhibit the nucleation and growth.

Non ionic surfactants are also widely used to control particle size and shape. For example, Pluronics P123, FC4 and Jeffamine compounds, make possible the access to smaller and more homogeneous particle size (150-300 nm) than when reductive additives are used. Materials prepared by using these surfactants present more homogeneous and smaller particles than those obtained with reductive agents. These surfactants can control particle size but do not decompose under reaction conditions, thus mild thermal treatments are needed in order to decompose them to carbon [Nazar, L.F. et al. (2007)].

On the other hand, the use of mixed water/solvent systems can also lead to the formation of diverse nanostructures. The solvent usually employed for this purpose is an alcohol. For example, an ethyleneglycol/water (EG/W) system has been developed to synthesize LiFePO$_4$ nanodendrites under hydrothermal conditions using dodecylbenzenesulphonicacid sodium salt (SDBS) as soft template to control crystal growth [Teng, F. et al. (2010)]. The advantages of this kind of synthetic approach are: one-step synthesis, environmental friendliness and low cost, due to the inexpensive solvent, as well as the short heating time used. This EG/W system is a promising reaction medium to provide well controlled crystallization, but the optimal EG/W proportion must be fixed for each desired compound because a too high proportion of ethyleneglycol should provoke only a partial solubility of the initial reactants. The role of the EG/W mixture is matching the reactivity of the precursors, which facilitates the formation of the desired olivine LiFePO$_4$ structure instead of impurity crystals, such as Li$_3$PO$_4$ and Fe$_4$(PO$_4$)$_3$(OH)$_3$. Moreover, the solubility of the precursors in EG/W will be smaller than the solubility in deionized water. Thus, the precursors will have a higher degree of supersaturation in the EG/W system, favouring the nucleation and growth of the desired crystals.

Surfactant in the system is used to adjust the size and morphology of the particle. SDBS molecules strongly coordinate onto the newly formed surfaces during crystallization and accordingly inhibit the crystal growth along these surfaces [Xiang, J. et al. (2008); Zhou, G. et al. (2007); Huang, Y. et al. (2009); Leem, G. et al. (2009)]. The proposed formation mechanism is depicted in figure 7.
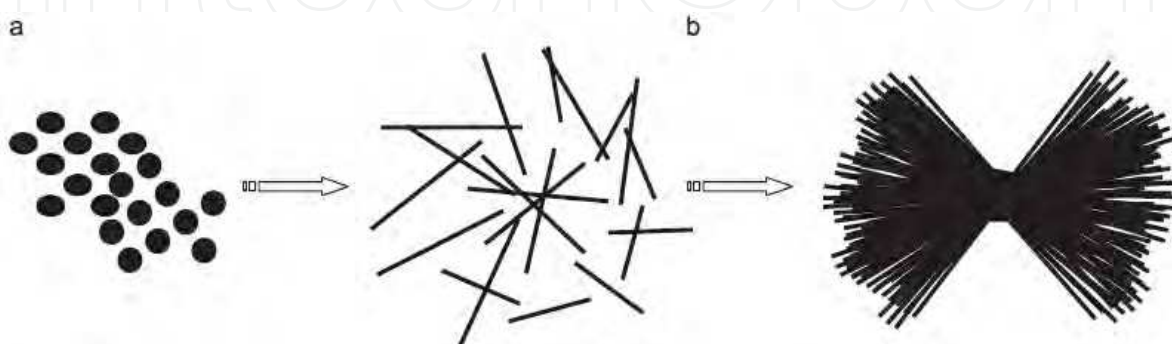

Fig. 7. The formation mechanism of the nanodendrites: a) particle growth and b) self-assembly by an end-to-end mode. (Reproduced from Teng, F. et al. (2010)).

During crystal growth, the surfactant acts as strong coordinating agent by binding to some crystal faces, and accordingly inhibits the crystal growth along the other defined crystal plane. As a result, at the early stages of the process, SDBS directs crystals to grow along the crystal direction whose crystal plane weakly bonds with the surfactant molecules. As a result, nanorods are formed. SDBS molecules can also act as soft template to assemble the nanorod building blocks into the final hierarchical structures, in which the nanorods are tightly attached together by their ends. This end-to end self-assembly results from the Van der Waals attraction of hydrophobic interaction on the surfactant molecules bonded to the end of the nanorods. Since surfactant molecules are preferentially and strongly adsorbed on the nanorod side, the stronger electrostatic force exists on the nanorod side than that on the end. It seems that there is a balance between electrostatic repulsion interaction and hydrophobic attraction interaction. Hence, the electrostatic repulsion interaction on the side is stronger than that on the end between nanorods, which refrains the side-by-side attachment. The long hydrophobic chains of the SDBS molecules bond on the nanorods will be attracted to one another through hydrophobic interaction. As a result, the nanorods are attached with each other by their ends to form hierarchical structures.
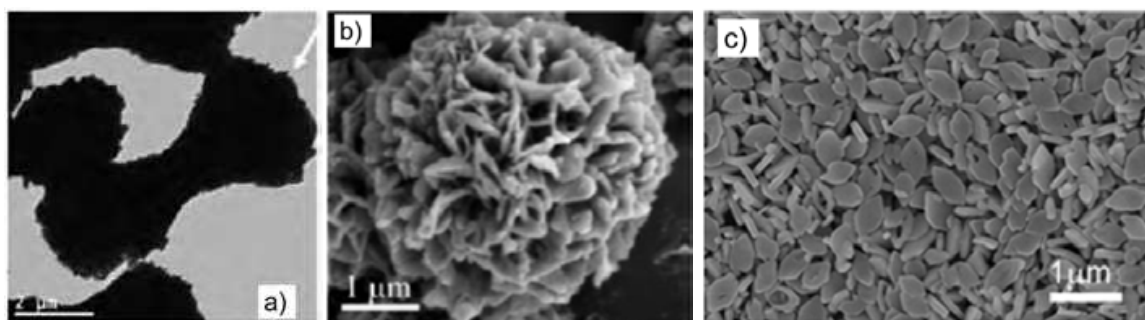

Fig. 8. Micrographs of different hierarchical structures prepared by solvothermal method, a) from ref. [Teng, F. et al. (2010), b) from Sun, C. et al. (2011), and c) is from Yang, S. et al. (2010).

An EG/W system has also been recently employed for the synthesis of porous LiFePO$_4$ microspheres by Goodenough's group in the presence of ethylenediamine [Sun, C. et al. (2011)]. In this case, ethyleneglycol/water ratio was 1/14, thus water was the main reaction medium. The role of EG in this solvothermal process consisted on limiting particle growth and preventing the agglomeration by means of chelates of EG (complexing agent) and on reducing Fe^{3+} into Fe^{2+} ions in solution (reductive agent). The presence of ethylenediamine as cosolvent in low concentration demonstrated to be critical for the formation of hierarchical flowerlike microspheres. Due to its strong chelating ability for some transition-metal ions, ethylenediamine has a great influence on the release of isolated iron ions, and, thus, on crystal growth. As-prepared hierarchical structures showed very good electrochemical properties, with a specific capacity value of 90 mAh·g^{-1} at 5C.

Polyethylene glycol/water (PEG/W) is another binary system that has been used to prepare electrode materials for Li ion batteries [Yang, S. et al. (2010)]. The use of different PEG/water proportions, heating temperatures (140º C and 180º C) and synthesis times (9-24 hours) leads to several morphologies, such as rod-like nanoparticles (50x200nm), nanoplates (100 nm thick and 800 nm long) and microplates (300 nm thick and 3μm long). Electrochemical evaluation of nanoplates showed very good results, with a specific capacity of 120-110 mAh·g^{-1} at 20C for 1000 cycles.

Anhydrous solvothermal processes also play an important role on the growth of hierarchically assembled nanostructures. Most of solvothermal systems are based on organic alcohols with different carbon chains. For example, benzyl alcohol has been reported in the last years to achieve nanostructures by solvothermal synthesis [Jia, F. et al. (2008); Pinna, N. et al. (2005)]. Benzyl alcohol and poly(vinyl pyrrolidone) (PVP) have been used to prepare $LiFePO_4$ dumb-bell structures, starting from an Fe^{3+} precursor [Yang, H. et al. (2009)]. Although benzyl alcohol is a reduced solvent that can partly reduce transition-metal ions [Niederberger, M. (2007)], the addition of LiI to the starting reactants is needed to accomplish complete reduction of Fe^{3+} to Fe^{2+} by I^- species. This way, benzyl alcohol provides a reductive environment and ensures reduction started with LiI. The role of PVP is related to the construction of the hierarchically self-assembled microstructures, and the adjustment of the amount of PVP is crucial to control both the morphology and size of the $LiFePO_4$ microstructures. The proposed mechanism for the formation of these dumb-bell structures is based on a dissolution-recrystallization process and it involves five steps (figure 9). The first one is the massive precipitation of Li_3PO_4 nuclei during the mixing of the reactants and the growth of the crystals in the shape of a rectangle. Second, the crystals start to aggregate in a system energy minimization driven process, and with the guide of PVP molecules, that bond to some crystal faces. Third, aggregation continues in an oriented way, to form pseudocubic 3C structure to minimize surface energy. Fourth, with increasing temperature and pressure, solubility of Li_3PO_4 increases and this phase starts to dissolve in order to crystallize $LiFePO_4$ nuclei. Driven by energy minimization principle, initial $LiFePO_4$ nanoplates assemble in edge to edge and layer-by-layer mode, and then, piled-up nanoplates tend to tilt at both ends, thus forming notched structures. This specific growth fashion can be due to lattice tension or surface interaction in the edge areas. Fifth, dissolution and recrystallization process complete by assembling more nanoplates onto the edges of the notched structures; these edges thicken and dumb-bell structures are formed. These nanostructures have not been electrochemically tested at high rates, and a 110 mAh·g^{-1} specific capacity value is obtained when cycling at C/30.
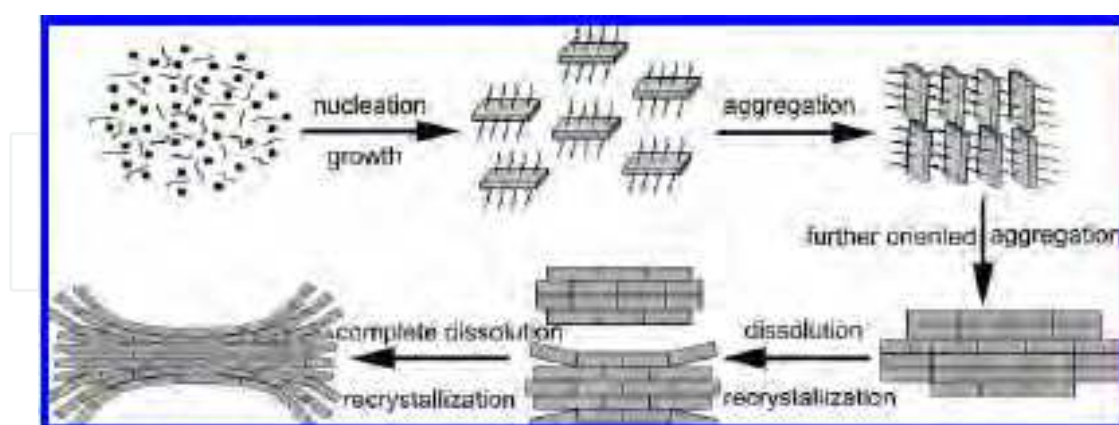

Fig. 9. Schematic illustration for the formation of hierarchically dumbbell-like $LiFePO_4$ microstructures. (Reproduced from ref Yang, H. et al. (2009)).

Ethylene glycol is the other alcohol largely used in solvothermal processes, not only combined with water, but also in anhydrous media, mixed with different surfactants or capping agents. $LiFePO_4$ nanorods and nanoflowers have been built by using this product as solvent, with short heating times (4-15 minutes) and relatively low temperature of 300º C

[Rangappa, D. et al. (2010)]. Three solvent combinations were tested, which induced different morphologies. When only EG was used as solvent, rectangular nanoplates of 50-100 nm width were produced. When EG and hexane were combined as solvent and cosolvent, long nanorods with 150 nm diameter and 700 nm long were obtained. In the case of using EG and oleic acid as solvent and surfactant, short nanorods were produced. In this last case, an increase in the reaction time provoked hierarchically self-assembly of the nanorods to form flower-like structures. Time-dependent experiments on EG-oleic acid system showed reaction sequence (figure 10). At first, $LiFePO_4$ spheres are formed. These spheres grow oriented to form rod-like structures, due to ethylene glycol, that directs the one dimensional growth by forming hydrogen bonds with certain faces of the crystals. With increasing reaction time, oleic acid molecules adsorb onto the surface of the nanorods, acting as a capping agent and also as a surfactant. The interaction of these oleic acid molecules leads to the decrease in the rods length and forms hierarchically flower like microstructure with prolonged reaction time. Electrochemical tests of these nanostructures showed a specific capacity of 154 mAh·g^{-1} at C/10.

A wide sloping region is usually observed in most hierarchically nanostructured materials. This can be attributed to a pseudo-capacitive effect, which consists on charge storage of Li ions from faradaic processes occurring at the surface of the materials. The presence of this kind of effect in hierarchically nanostructured materials makes sense in samples with great specific surface, such as nanoflowers.
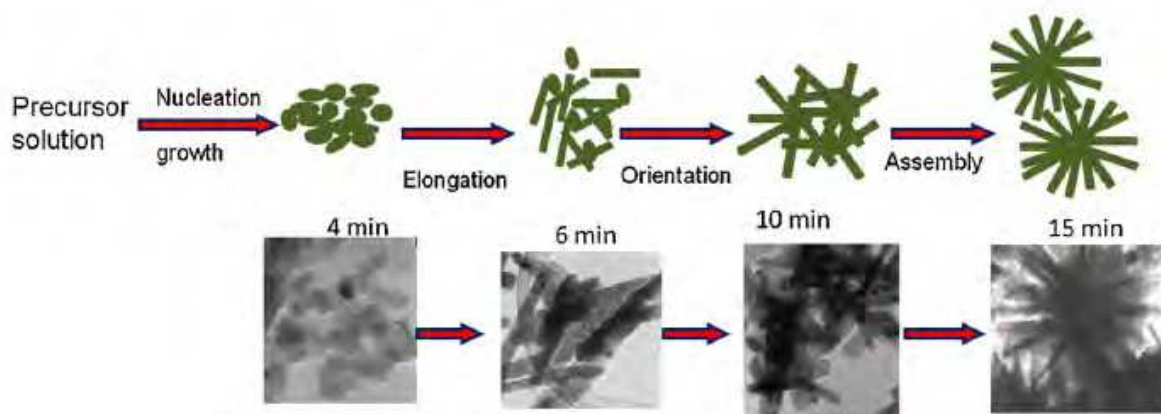

Fig. 10. Schematic illustration of the directed growth of $LiFePO_4$ nanorods and 3D hierarchical nanoflower by nanorods self-assembly. (Reproduced from Rangappa, D. et al. (2010))

3.4 Synthesis of nanostructured materials by ionothermal process

New synthetic methods derived from solvothermal approach, such as ionothermal processes have been used to obtain nanopowders of $LiMPO_4$ (M= Mn, Co and Ni), Li_xMSiO_4 [Nytén, A. et al. (2005)] and Li and Na fluorophosphates battery materials [DiSalvo, F.J. et al. (1971); Ellis, B.L. et al. (2007b)] using low heating temperature. Ionothermal synthesis has emerged when a great amount of research work is aimed at new low-cost processes to make highly electrochemically optimized electrode materials. This alternative route is considered as a new low cost synthesis process because it demands much less energy than high temperature ceramic routes. In spite of the higher cost of ionic liquids compared to water, it

has been proved that these solvents can be reused without purification when used to prepare the same material, what leads to a significant cost decrease and minimizes waste production [Tarascon, J-M. et al. (2010)]. Ionothermal synthesis has also been carried out successfully by using microwave rather than traditional heating, which reduces reaction time and required energy for the synthesis.

Ionothermal synthesis is based on the use of an ionic liquid as reacting medium instead of water in solvothermal conditions. Ionic liquids are a class of organic solvents with high polarity and a preorganized solvent structure [Del Popolo, M. G. and Voth, G. A. (2004)]. Room temperature (or near-room-temperature) ionic liquids are classically defined as liquids at ambient temperatures (or <100 °C) that are made of organic cations and anions. They have excellent solvating properties, little measurable vapor pressure, and high thermal stability. Solvating properties and fusion temperatures will depend on the combination of cations and anions chosen. In the area of materials science, there have been several reports of ionic liquids being used as solvents with very little or controlled amounts of water involved in the synthesis [Antonietti, M et al. (2004)]. Most of these studies concentrated on amorphous materials and nanomaterials.

Like water, ionic liquids resulting from compatible cationic/anionic pairs have excellent solvent properties. In addition, they possess high thermal stability and negligible volatility so the use of autoclave is not mandatory. Moreover, because of the flexible nature of the cationic/anionic pairs, they present, as solvents, great opportunities to purposely direct nucleation. Over the past decade, ionothermal synthesis has developed into an advantageous synthetic technique for the preparation of zeotypes [Lin, Z-J. et al. (2008)] and other porous materials such as metal organic framework compounds (MOFs), but there has been very limited use made of this technique in the synthesis of inorganic compounds.

The unique feature of ionothermal synthesis is that the ionic liquid acts as both the solvent and the template provider. Many ionic liquid cations are chemically very similar to species that are already known as good templates (alkylimidazolium-based, pyridinium-based ionic liquids). Many are relatively polar solvents, making them suitable for the dissolution of the inorganic components required for the synthesis. One of the defining properties of ionic liquids is their lack of a detectable vapor pressure which effectively results in the elimination of the safety concerns associated with high hydrothermal pressures and has also led to their use in microwave synthesis.

In the process of ionothermal route, since there are no other solvents added to the reaction mixture, the theory holds that no other molecules are present to act as space fillers during the synthesis. This means that ionothermal method ideally removes the competition between template–framework and solvent–framework interactions that are present in hydrothermal preparations. This, however, is the idealistic scenario, which is not always attainable due to the possible decomposition of a small fraction of the ionic liquid cations, resulting in smaller template cations which may preferentially act as the structure directing agent in the ionic liquid solvent [Parnham, E. R. and Morris, R. E. (2006)].

Recent molecular modeling studies indicate that the structures of ionic liquids are characterized by long range correlations and distributions that reflect the asymmetric structures of the cations. Long-range asymmetric effects of this kind potentially increase the likelihood of transferring chemical information from the template cation to the framework, a situation that is desirable if full control over the templating process is to be achieved [Parnham, E.R. and Morris, R.E. (2007)].

Compound	Precursors	Ionic Liquids	Particle size (nm)
$LiFePO_4$	LiH_2PO_4 + $FeC_2O_4 \cdot 2H_2O$	EMI-TFSI 1-ethyl-3-methylimidazolium Bis(trifluoromethanesulfonyl)imide	150-300
$LiMnPO_4$	LiH_2PO_4 + $MnC_2O_4 \cdot 2H_2O$	EMI-TFSI 1-ethyl-3-methylimidazolium Bis(trifluoromethanesulfonyl)imide	100-400
$LiMPO_4$ (M= Ni, Co)	LiH_2PO_4 + $MC_2O_4 \cdot 2H_2O$	EMI-TFSI 1-ethyl-3-methylimidazolium Bis(trifluoromethanesulfonyl)imide	800-1000
Na_2FePO_4F	Na_3PO_4+ $FeF_2/FeCl_2$	C2 1-butyl-2,3-dimethylimidazolium Bis(trifluoromethanesulfonyl)imide	<50
Na_2MnPO_4F	Na_3PO_4+ $MnF_2/MnCl_2$	C2 1-butyl-2,3-dimethylimidazolium Bis(trifluoromethanesulfonyl)imide	<50
$Na_2Fe_{1-x}Mn_xPO_4F$ $(0 \le x \le 0.15)$	Na_3PO_4+ $MnF_2/MnCl_2$	C2 1-butyl-2,3-dimethylimidazolium Bis(trifluoromethanesulfonyl)imide	<50
$Na_2Fe_{1-x}Mn_xPO_4F$ $(0.25 \le x \le 1)$	Na_3PO_4+ $MnF_2/MnCl_2$	C2 1-butyl-2,3-dimethylimidazolium Bis(trifluoromethanesulfonyl)imide	<50
$LiFePO_4F$	Li_3PO_4+FeF_3	Triflate 1-butyl-3-methylimidazolium Trifluoromethanesulfonate	<50
$LiTiPO_4F$	Li_3PO_4+TiF_3	C2-OH 1,2-dimethyl-3-(3-hdroxypropyl)-imidazolium Bis(trifluoromethanesulfonyl)imide	<50
$LiFeSO_4F$	$FeSO_4 \cdot H_2O$+LiF	EMI-TFSI 1-ethyl-3-methylimidazolium Bis(trifluoromethanesulfonyl)imide	600-1200
$LiMnSO_4F$	$MnSO_4 \cdot H_2O$+LiF	EMI-TFSI 1-ethyl-3-methylimidazolium Bis(trifluoromethanesulfonyl)imide	600-1200

Table 1. List of compounds prepared by ionothermal process with different ionic liquids [Tarascon, J-M. et al. (2010)].

Tarascon et al. were the first to apply ionothermal synthesis to battery electrode materials. They tested several ionic liquids based on different cationic and anionic species as reacting medium for the preparation of $LiFePO_4$ phase [Recham, N. et al. (2009a)]. The ionic liquids used demonstrated to have an impact on $LiFePO_4$ nucleation/growth and to behave as a structural directing agent. For example, the use of a CN functionalized EMI-TFSI ionic liquid [1-ethyl-3-methylimidazolium bis(trifluoromethanesulfonyl)imide] produced needle-like powders along [010] direction that perfectly piled up to form a larger needle. This change on the ending group modified the polar character of the reacting medium and its solvating

properties, thus, influencing crystal growth. Platelet-like particles along [020] direction were created by decreasing the polarity via the use of a C_{18}-based EMI cation. Formation of these two morphological kinds can be explained in terms of competing energy surfaces, and it is directly connected with the nature of the ionic liquid, solvating power, polarity and aptitude to specifically absorb on one of the surfaces. Depending on the ionic liquid properties, surface energy minimization of the system will take place via a different mechanism. All $LiFePO_4$ produced materials were electrochemically active, but those with the best performance were of 300 and 500 nm size, showing 150 mAh·g^{-1} specific capacity at C/10 without carbon coating.

Ionothermal process was extended to the synthesis of size-controlled Na-based fluorophosphates [Na_2MPO_4F (M= Fe, Mn)] [Recham, N. et al. (2009b)]. These phases are attractive electrode materials because they are based on economic metals and can be used in both Li- and Na-based batteries. Furthermore, the fluorides possess higher electronegativity which increases the ionicity of the bonds and, thus, their redox potentials due to inductive effect. Nanosized samples of Na_2FePO_4F and Na_2MnPO_4F of about 25 nm diameter were prepared in a 1,2-dimethyl-3-butylimidazolium bis(trifluoromethanesulfonyl imide) ionic liquid, in contrast with coarse powders obtained by ceramic method. Electrochemical performance of the iron compound reached better results than that of ceramic material, with 115 mAh·g^{-1}, better initial capacity, lower irreversible capacity, lower polarization and better capacity retention. Manganese phase did not show electrochemical activity, which follows the general tendency of Mn-based compounds having worse electrochemical performance than their Fe counterpart, for example in $LiMPO_4$ and Li_2MSiO_4 families. There are two factors related to this phenomenon. First, the strong Jahn-Teller distortion on Mn^{3+}, that affects its coordination sphere; and, second, the poor electronic-ionic conductivity of the materials, owing to the greater ionicity of the M-O bonding.

Ionothermal process has been successfully used for preparing new electroactive materials that had not been achieved before, such as $LiFeSO_4F$. This material possesses an adequate structure to favor Li ions migration along channels. This electroactive phase had not been synthesized before because it is not accessible, neither by ceramic process nor in water medium. It decomposes at temperatures beyond 375º C and in water medium. This new cathode material showed electrochemical activity at 3.6 V, and a reversible specific capacity of 140 mAh·g^{-1}, very close to theoretical specific capacity vale of 151 mAh·g^{-1}. Thus, this preparative process has demonstrated to be a useful tool to synthesize nanosized new and known electroactive materials.

3.5 Synthesis of nanostructured materials with biological agents

The latest trend in battery materials processing is using biomineralization process in order to build controlled nanoarchitectured compounds under ambient conditions [Ryu, J. et al. (2010)]. Biomimetic chemistry involves the utilization of actual biomolecular entities such as proteins, bacteria and viruses to act either as a growth medium or as a spatially constrained nanoscale reactor for the generation of nanoparticles. Biosystems have the inherent capabilities of molecular recognition and self-assembly, and thus are an attractive template for constructing and organizing the nanostructure. Ryu et al. synthesized nanostructured transition metal phosphate via biomimetic mineralization of peptide nanofibers (figure 11). Peptides self-assembled into nanofibers displaying numerous acidic and polar moieties on their surface and readily mineralized with transition metal phosphate by sequential

treatment with aqueous solutions containing transition metal cations and phosphate anions. $FePO_4$-mineralized peptide nanofibers were thermally treated at 350° C to fabricate $FePO_4$ nanotubes with inner walls coated with a thin layer of conductive carbon by carbonization of the peptide core. As formed carbon coated $FePO_4$ nanotubes showed high reversible capacity (150 mAh·g^{-1} at C/17) and good capacity retention during cycling.
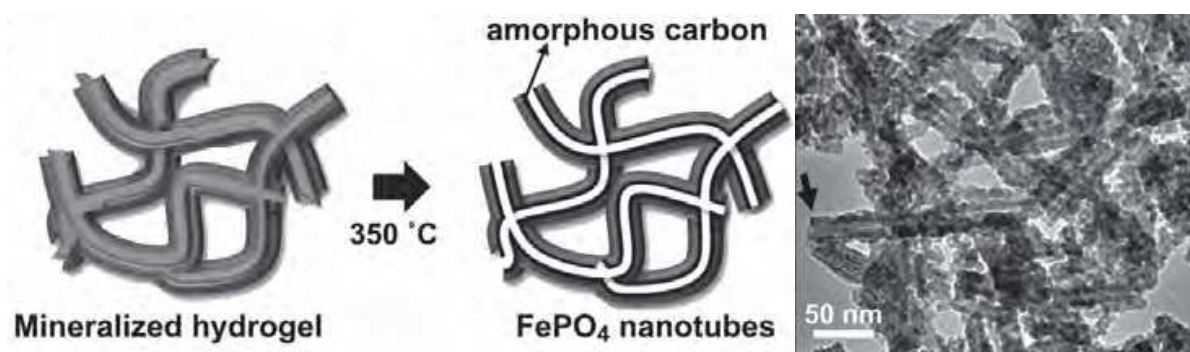

Fig. 11. a) Schematic of $FePO_4$ nanotubes synthesis by heat treatment of peptide/$FePO_4$ hybrid nanofibers; and b) transmission micrograph of tubular structures. [Reproduced from Ryu et al. (2010)].

Bacillus pasteurii bacterium has been extensively used to provoke calcite precipitation and it can generate a basic medium from urea hydrolysis that helps growing of $LiFePO_4$ nanofilaments at 65° C. Beer yeast has also been reported as a biomimetic template that has been used to prepare $LiFePO_4$ with enhanced surface area and conductivity [Li, P. et al. (2009)]. Engineered viruses have also been reported as templates to synthesize various electrode materials [Mao, Y. et al. (2007)], such as gold-cobalt oxide nanowires that consisted on 2-3 nm diameter nanocrystals prepared with modified bacteria M13 virus, with enhanced capacity retention [Tam, K.T. et al. (2006)]. Tobacco mosaic virus has also been used as a template for the synthesis of nickel and cobalt surfaces. This virus was genetically engineered to express a novel coat protein cysteine residue, and to vertically pattern virus particles into gold surfaces via gold-thiol interactions. Gold-supported vertically aligned virion particles served as vertical templates for reductive deposition of Ni and Co at room temperature via electroless deposition, and thus produced high surface area electrodes [Royston, E. et al. (2008)].

4. Conclusions

Nanostructure and hierarchical growth of electroactive materials has led to enhanced performances of lithium ion rechargeable cells such as higher capacity, improved rate capability, and sustained capacity retention for longer cycles. The key feature for the achievement of this goal has been the evolution of synthetic methods. From the classical ceramic to more advanced solvothermal processes, or to interdisciplinary views such as the use of biological agents to produce electrode materials, it is clear that, at present, synthetic approaches must go beyond the limits of traditional methods and set up a continuous knowledge feedback with surrounding disciplines in order to find new synthetic routes that lead to better performing materials and, thus, to a better quality of life.

The control of reaction conditions by using nano-shaped precursors, hard or soft templates or agents to limit the growth of particles allows the creation of useful featured structures that are able to overcome typical problems in battery materials.

5. Acknowledgements

6. References

Antonietti, M; Kuang, D.; Smarsly, B. & Zhou, Y. (2004) Ionic liquids for the convenient synthesis of functional nanoparticles and other inorganic nanostructures. *Angew. Chem.*, Vol. 43, pp. 4988– 4992, ISSN 1521-3773.

Aragón, M.J.; Lavela, P.; León, B.; Pérez-Vicente, C.; Tirado, J. L. & Vidal-Abarca, C. (2010) On the use of the reverse micelles synthesis of nanomaterials for lithium-ion batteries. *J. Solid State Electrochem.*, Vol. 14, pp. 1749-1753, ISSN 1432-8488.

Baythoun, M.S.G. & Sale, F.R. (1982) Production of strontium-substituted lanthanum manganite perovskite powder by the amorphous citrate process. *J. Mater. Sci.*, Vol. 17, pp. 2757-2769, ISSN 1573-4803.

Beninati, S.; Damen, L. & Mastragostino, M. (2008) MW-assisted synthesis of $LiFePO_4$ for high power applications. *J. Power Sources*, Vol. 180, pp. 875-879, ISSN 0378-7753.

Bruce, P.G. (2008a) Energy storage beyond the horizon: Rechargeable lithium batteries. *Solid State Ionics*, Vol. 179, pp. 752-760, ISSN 0167-2738.

Bruce, P.G.; Scrosati, B. & Tarascon, J-M. (2008b) Nanomaterials for Rechargeable Lithium Batteries. *Angew. Chem. Int. Ed.*, Vol. 47, pp. 2930-2946, ISSN 1521-3773.

Chen, J. and Whittingham, M.S. (2006) Hydrothermal synthesis of lithium iron phosphate. *Electrochem. Commun.*, Vol. 8, pp. 855-858, ISSN 1388-2481.

Chen, J.; Wang, S. & Whittingham, M.S. (2007) Hydrothermal synthesis of cathode materials. *J. Power Sources*. Vol. 174, pp. 442-448, ISSN 0378-7753.

Cho, Y. & Cho, J. (2010) Significant Improvement of $LiNi_{0.8}Co_{0.15}Al_{0.05}O_2$ Cathodes at 60°C by SiO_2 Dry Coating for Li-Ion Batteries. *J. Electrochem. Soc.*, Vol. 157, pp. A625-A629, ISSN 0013-4651.

Choi, D. & Kumta, P.N. (2007) Surfactant based sol–gel approach to nanostructured $LiFePO_4$ for high rate Li-ion batteries. *J. Power Sources*, Vol. 163, pp. 1064-1069, ISSN 0378-7753.

Chung, H-T.; Jang, S-K.; Ryu, H. W. & Shim, K-B. (2004) Effects of nano-carbon webs on the electrochemical properties in $LiFePO_4$/C composite. *Solid State Commun.*, Vol. 131, pp. 549-554, ISSN 0038-1098.

Del Popolo, M. G. & Voth, G. A. (2004) On the structure and dynamics of ionic liquids. *J. Phys. Chem. B*, Vol. 108, pp.1744–1752, ISSN 1520-5207.

Delacourt, C.; Poizot, P.; Levasseur, S. & Masquelier, C. (2006) Size Effects on Carbon-Free $LiFePO_4$ Powders: The Key to Superior Energy Density. *Electrochem. Solid State Lett.*, Vol. 9, pp. A352-A355, ISSN 1099-0062.

DiSalvo, F.J.; Schwall, R.; Geballe, T. H.; Gamble, F. R. & Osiecki, J. H. (1971) Superconductivity in layered compounds with variable interlayer spacings. *Phys. Rev. Lett.*, Vol. 27, pp. 310-313, ISSN 0031-9007.

Doherty, C.M.; Caruso, R. A.; Smarsly, B. M. & Drummond, C. J. (2009) Colloidal Crystal Templating to Produce Hierarchically Porous $LiFePO_4$ Electrode Materials for High Power Lithium Ion Batteries. *Chem. Mater.*, Vol. 21, pp. 2895-2903, ISSN 0897-4756.

Dokko, K.; Koizumi, S.; Nakano, H. & Kanamura, K. (2007) Particle morphology, crystal orientation, and electrochemical reactivity of $LiFePO_4$ synthesized by the hydrothermal method at 443 K. *J. Mater. Chem.*, Vol. 17, pp. 4803-4810, ISSN 0959-9428.

Ellis, B.; Kan, W. H.; Makahnouk, W. R. M. & Nazar, L. F. (2007a) Synthesis of nanocrystals and morphology control of hydrothermally prepared $LiFePO_4$. *J. Mater. Chem.* Vol. 17, pp. 3248-3254, ISSN: 0959-9428.

Ellis, B.L.; Makahnouk, W. R. M.; Makimura, Y.; Toghill, K. & Nazar, L. F. (2007b) A multifunctional 3.5 V iron-based phosphate cathode for rechargeable batteries. *Nat. Mater.*, Vol. 6, pp. 749-753, ISSN 1476-1122.

Eom, J.; Ryu, K.S. & Cho, J. (2008) Dependence of Electrochemical Behavior on Concentration and Annealing Temperature of Li_xCoPO_4 Phase-Grown $LiNi_{0.8}Co_{0.16}Al_{0.04}O_2$ Cathode Materials. *J. Electrochem. Soc.*, Vol. 155, pp. A228-A233, ISSN 0013-4651.

Hsu, K-F.; Tsay, S-Y. & Hwang, B-J. (2004) Synthesis and characterization of nano-sized $LiFePO_4$ cathode materials prepared by a citric acid-based sol–gel route. *J. Mater. Chem.*, Vol. 14, pp. 2690-2695, ISSN 0959-9428.

Huang, Y.; Wang, W.; Liang, H. & Xu, H. (2009) Surfactant-Promoted Reductive Synthesis of Shape-Controlled Gold Nanostructures. *Cryst. Growth Des.*, Vol. 9, pp. 858-862, ISSN 1528-7483.

Hwang, B-J.; Hsu, K-F.; Hu, S-K; Cheng, M-Y.; Chou, T-C.; Tsay, S-Y. & Santhanam, R. (2009) Template-free reverse micelle process for the synthesis of a rod-like $LiFePO_4/C$ composite cathode material for lithium batteries. *J. Power Sources*, Vol. 194, pp. 515-519, ISSN 0378-7753.

Jia, F.; Zhang, L. Z.; Shang, X. Y. & Yang, Y. (2008) Non-Aqueous Sol–Gel Approach towards the Controllable Synthesis of Nickel Nanospheres, Nanowires, and Nanoflowers. *Adv. Mater.*, Vol. 20, pp.1050-1054, ISSN 1521-4095.

Jiao, F.; Shaju, K. M. & Bruce, P. G. (2005) Synthesis of Nanowire and Mesoporous Low-Temperature $LiCoO_2$ by a Post-Templating Reaction. *Angew. Chem. Int. Ed.*, Vol. 44, pp. 6550-6553, ISSN 1521-3773.

Jin, B. & Gu, H-B. (2008) Preparation and characterization of $LiFePO_4$ cathode materials by hydrothermal method. *Solid State Ionics*, Vol. 178, pp. 1907-1914, ISSN 0167-2738.

Kanamura, K. & Koizumi, S. (2008) Hydrothermal synthesis of $LiFePO_4$ as a cathode material for lithium batteries. *J. Mater. Sci.*, Vol. 43, pp. 2138-2142, ISSN 1573-4803.

Kim, C.W.; Lee, M.H.; Jeong, W.T. & Lee, K.S. (2005) Synthesis of olivine $LiFePO_4$ cathode materials by mechanical alloying using iron(III) raw material. *J. Power Sources*, Vol. 146, pp. 534-538, ISSN 0378-7753.

Kim, J-K.; Choi, J-W.; Cheruvally, G.; Kim, J-U.; Ahn, J-H.; Cho, G-B.; Kim, K-W. & Ahn, H-J. (2007) A modified mechanical activation synthesis for carbon-coated $LiFePO_4$ cathode in lithium batteries. *Matter. Lett.*, Vol. 61, pp. 3822-3825, ISSN 0167-577X.

Kim, D.H. & Kim, J. (2007) Synthesis of $LiFePO_4$ nanoparticles and their electrochemical properties. *J. Phys. Chem. Solids*, Vol. 68, pp. 734-737, ISSN 0022-3697.

Kwon, S.J.; Kim, C.W.; Jeong, W.T. & Lee, K.S. (2004) Synthesis and electrochemical properties of olivine $LiFePO_4$ as a cathode material prepared by mechanical alloying. *J. Power Sources*, Vol. 137, pp. 93-99, ISSN 0378-7753.

Leem, G.; Sarangi, S.; Zhang, S.; Rusakova, I.; Brazdeikis, A.; Litvinov, D. & Lee, T. R. (2009) Surfactant-Controlled Size and Shape Evolution of Magnetic Nanoparticles. *Cryst. Growth Des.*, Vol. 9, pp. 32-34, ISSN 1528-7483.

Li, M.; Schnablegger, H. & Mann, S. (1999) Coupled synthesis and self-assembly of nanoparticles to give structures with controlled organization. *Nature*, Vol. 402, pp. 393-395, ISSN 0028-0836.

Li, W.; Ying, J.; Wan, C.; Jiang, C.; Gao, J. & Tang, C. (2007) Preparation and characterization of $LiFePO_4$ from $NH_4FePO_4 \cdot H_2O$ under different microwave heating conditions. *J. Solid State Electrochem.*, Vol. 11, pp. 799-803, ISSN 1432-8488.

Li, P.; He, W.; Zhao, H. & Wang, S. (2009) Biomimetic synthesis and characterization of the positive electrode material $LiFePO_4$. *J. Alloys and Comp.*, Vol. 471, pp. 536-538, ISSN 0925-8388.

Liao, X.Z.; Ma, Z-F.; He, Y-S.; Zhang, X-M.; Wang, L. & Jiang, Y. (2005) Electrochemical Behavior of $LiFePO_4$/C Cathode Material for Rechargeable Lithium Batteries. *J. Electrochem. Soc.*, Vol. 152, pp. A1969-A1973, ISSN 0013-4651.

Lin, Z-J.; Alexandra, Y. L.; Slawin, M. Z. & Morris, R. E. (2008) Hydrogen-bond-directing effect in the ionothermal synthesis of metal coordination polymers. *Dalton Trans.*, pp. 3989-3994, ISSN 1364-5447.

Mao, Y.; Park, T-J.; Zhang, F.; Zhou, H. & Wong, S. S. (2007) Environmentally Friendly Methodologies of Nanostructure Synthesis. *Small*, Vol. 3, pp.1122-1139, ISSN 1613-6810.

Mi, C.H.; Zhao, X. B.; Cao, G. S. & Tu, J. P. (2005) *In Situ* Synthesis and Properties of Carbon-Coated $LiFePO_4$ as Li-Ion Battery Cathodes. *J. Electrochem. Soc.*, Vol. 152, pp. A483-A487, ISSN 0013-4651.

Mi, C.H.; Cao, G.S. & Zhao, X.B. (2005) Low-cost, one-step process for synthesis of carbon-coated $LiFePO_4$ cathode. *Matter. Lett.*, Vol. 59, pp.127-130, ISSN 0167-577X.

Nakamura, T.; Miwa, Y.; Tabuchi, M. & Yamada, Y. (2006) Structural and Surface Modifications of $LiFePO_4$ Olivine Particles and Their Electrochemical Properties. *J. Electrochem. Soc.*, Vol. 153, pp. A1108-A1114, ISSN 0013-4651.

Niederberger, M. (2007) Nonaqueous Sol-Gel Routes to Metal Oxide Nanoparticles. *Acc. Chem. Res.*, Vol. 40, pp. 793-800, ISSN 1520-4898.

Nytén, A.; Abouimrane, A.; Armand, M.; Gustafsson, T. & Thomas, J. O. (2005) Electrochemical performance of Li_2FeSiO_4 as a new Li-battery cathode material. *Electrochem. Commun.*, Vol. 7, pp. 156-160, ISSN 1388-2481.

Palomares, V. Goñi, A.; Gil de Muro, I.; de Meatza, I.; Bengoechea, M.; Miguel, O. & Rojo, T. (2007) New freeze-drying method for $LiFePO_4$ synthesis. *J. Power Sources*, Vol. 171, pp. 879-885, ISSN 0378-7753.

Palomares, V.; Goñi, A.; Gil de Muro, I.; de Meatza, I.; Bengoechea, M.; Cantero, I. & Rojo, T. (2009a) Influence of Carbon Content on $LiFePO_4$/C Samples Synthesized by Freeze-Drying Process. *J. Electrochem. Soc.*, Vol. 156, pp. A817-A821, ISSN 0013-4651.

Palomares, V.; Goñi, A.; Gil de Muro, I.; de Meatza, I.; Bengoechea, M.; Cantero, I. & Rojo, T. (2009b) Conductive additive content balance in Li-ion battery cathodes: Commercial carbon blacks vs. *in situ* carbon from $LiFePO_4$/C composites. *J. Power Sources*, Vol. 195, pp. 7661-7668, ISSN 0378-7753.

Palomares, V.; Goñi, A.; Gil de Muro, I.; Lezama, L.; de Meatza, I.; Bengoechea, M.; Boyano, I. & Rojo, T. (2011) Near heterosite $Li_{0.1}FePO_4$ Phase Formation as Atmospheric Aging Product of $LiFePO_4$/C Composite. Electrochemical, Magnetic and EPR Study. *J. Electrochem. Soc.*, Vol. 158(9), pp. A1042-A1047, ISSN 0013-4651.

Park, K.S.; Son, J. T.; Chung, H. T.; Kim, S. J.; Lee, C. H.; & Kim, H. G. (2003) Synthesis of $LiFePO_4$ by co-precipitation and microwave heating. *Electrochem. Commun.*, Vol. 5, pp. 839-842, ISSN 1388-2481.

Park, K.S.; Kang, K.T.; Lee, S.B.; Kim, G.Y.; Park, Y.J. & Kim, H.G. (2004) Synthesis of LiFePO$_4$ with fine particle by co-precipitation method. *Mater. Res. Bull.*, Vol. 39, pp. 1803-1810, ISSN 0025-5408.

Parnham, E. R. & Morris, R. E. (2006) 1-Alkyl-3-methylimidazolium bromide ionic liquids in the ionothermal synthesis of aluminium phosphate molecular sieves. *Chem. Mater.*, Vol. 18, pp. 4882–4887, ISSN 0897-4756.

Parnham, E.R. & Morris, R.E. (2007) Ionothermal Synthesis of Zeolites, Metal–Organic Frameworks, and Inorganic– Organic Hybrids. *Acc. Chem. Res.*, Vol. 40, pp. 1005-1013, ISSN 1520-4898.

Paulus, M. (1980) Freeze-drying: a method for the preparation of fine sinterable powders and low temperature solid state reaction. *Fine Part. Process. Int. Symp.*, Vol. 1, pp. 27-50.

Pechini, P. Patent 3.330.697, July 11, 1967.

Piana, M.; Cushing, B.L.; Goodenough, J.B. & Penazzi, N. (2004) A new promising sol–gel synthesis of phospho-olivines as environmentally friendly cathode materials for Li-ion cells. *Solid State Ionics*, Vol. 175, pp. 233-237, ISSN 0167-2738.

Pieranski, P. (1983) Colloidal Crystals. *Contemp. Phys.*, Vol. 24, p.25-73, ISSN 0010-7514.

Pinna, N.; Grancharov, S.; Beato, P.; Bonville, P.; Antonietti, M. & Niederberge, M. (2005) Magnetite Nanocrystals: Nonaqueous Synthesis, Characterization, and Solubility. *Chem. Mater.*, Vol, 17, pp. 3044-3049, ISSN 0897-4756.

Rangappa, D.; Sone, K.; Kudo, T. & Honma, I. (2010) Directed growth of nanoarchitectured LiFePO$_4$ electrode by solvothermal synthesis and their cathode properties. *J. Power Sources*, Vol. 195, pp. 6167-6171, ISSN 0378-7753.

Recham, N.; Dupont, L.; Courty, M.; Djellab, K.; Larcher, D.; Armand, M. & Tarascon, J.-M. (2009a) Ionothermal Synthesis of Tailor-Made LiFePO$_4$ Powders for Li-Ion Battery Applications. *Chem. Mater.*, Vol. 21, pp. 1096-1107, ISSN 0897-4756.

Recham, N.; Chotard, J-N.; Dupont, L. ; Djellab, K.; Armand, M. & Tarascon, J-M. (2009b) Ionothermal Synthesis of Sodium-Based Fluorophosphate Cathode Materials. *J. Electrochem. Soc.*, Vol. 156, pp. A993-A999, ISSN 0013-4651.

Ryu, J.; Kim, S-W.; Kang, K. & Park, C. B. (2010) Mineralization of Self-assembled Peptide Nanofibers for Rechargeable Lithium Ion Batteries. *Adv. Mater.*, Vol 22, pp. 5537-5541, ISSN 0935-9648.

Royston, E.; Ghosh, A.; Kofinas, P.; Harris, M. T. & Culver, J. N. (2008) Self-Assembly of Virus-Structured High Surface Area Nanomaterials and Their Application as Battery Electrodes. *Langmuir*, Vol. 24, pp. 906-912, ISSN 1520-5827.

Sakamoto, J.S. & Dunn, B. (2002) Hierarchical battery electrodes based on inverted opal structures. *J. Mater. Chem.*, Vol. 12, pp. 2859-2861, ISSN 0959-9428.

Song, M-S.; Kang, Y.M.; Kim, J-H.; Kim, H-S.; Kim, D-Y.; Kwon, H-S. & Lee, J.Y. (2007) Simple and fast synthesis of LiFePO$_4$-C composite for lithium rechargeable batteries by ball-milling and microwave heating. *J. Power Sources*, Vol. 166, pp. 260-265, ISSN 0378-7753.

Song, M-S.; Kim, D-Y.; Kang, Y-M.; Kim, Y-I.; Lee, J-Y. & Kwon, H-S. (2008) Synthesis and characterization of Carbon Nano Fiber/LiFePO$_4$ composites for Li-ion batteries. *J. Power Sources*, Vol. 180, pp. 546-552, ISSN 0378-7753.

Song, H-K.; Lee, K.T.; Kim, M.G.; Nazar, L.F. & Cho, J. (2010) Recent Progress in Nanostructured Cathode Materials for Lithium Secondary Batteries. *Adv. Funct. Mater.*, Vol. 20, pp. 3818-3834, ISSN 1616-3028.

Sun, C.; Rajasekhara, S.; Goodenough, J. B. & Zhou, F. (2011) Monodisperse Porous LiFePO$_4$ Microspheres for a High Power Li-Ion Battery Cathode. *J. Am. Chem. Soc.*, Vol. 133, pp. 2132-2135, ISSN 0002-7863.

Tajimi, S.; Ikeda, Y.; Uematsu, K.; Toda, K. & Sato, M. (2004) Enhanced electrochemical performance of LiFePO$_4$ prepared by hydrothermal reaction. *Solid State Ionics*, Vol. 175, pp. 287-290, ISSN 0167-2738.

Tam, K.T.; Kim, D-W.; Yoo, P. J.; Chiang, C-Y.; Meethong, N.; Hammond, P. T.; Chiang, Y-M. & Belcher, A. M. (2006) Virus-Enabled Synthesis and Assembly of Nanowires for Lithium Ion battery Electrodes. *Science*, Vol. 312, pp. 885-888, ISSN 1095-9203.

Tarascon, J-M.; Recham, N.; Armand, M.; Chotard, J-N.; Barpanda, P.; Walker, W. & Dupont, L. (2010) Hunting for Better Li-Based Electrode Materials via Low Temperature Inorganic Synthesis. *Chem. Mater.*, Vol. 22, pp. 724-739, ISSN 0897-4756.

Teng, F.; Santhanagopalan, S.; Asthana, A.; Geng, X.; Mho, S-I.; Shahbazian-Yassar, R. & Meng, D. D. (2010) Self-assembly of LiFePO$_4$ nanodendrites in a novel system of ethyleneglycol–water. *J. Crystal Growth*, Vol. 312, pp. 3493-3502, ISSN 0022-0248.

Tonti, D.; Torralvo, M. J.; Enciso, E.; Sobrados, I. & Sanz, J. (2008) Three-Dimensionally Ordered Macroporous Lithium Manganese Oxide for Rechargeable Lithium Batteries. *Chem. Mater.*, Vol. 20, pp. 4783-4790, ISSN 0897-4756.

Velev, O.D.; Jede, T. A.; Lobo, R. F. & Lenhoff, A. M. (1997) Porous silica via colloidal crystallization. *Nature*, Vol. 389, pp. 447-448, ISSN 0028-0836.

Wang, L.; Huang, Y.; Jiang, R. & Jia, D. (2007) Preparation and characterization of nano-sized LiFePO$_4$ by low heating solid-state coordination method and microwave heating. *Electrochimica Acta*, Vol. 52, pp.6778-6783, ISSN 0013-4686.

Whittingham, M.S.; Song, Y.; Lutta, S.; Zavalij, P. Y. & Chernova, N. A. (2005) Some transition metal (oxy)phosphates and vanadium oxides for lithium batteries. *J. Mater. Chem.*, Vol. 15, pp. 3362-3379, ISSN 0959-9428.

Xiang, J.; Cao, H.; Warner, J. H. & Watt, A. A. R. (2008) Crystallization and Self-Assembly of Calcium Carbonate Architectures. *Cryst. Growth Des.*, Vol. 8, pp. 4583-4588, ISSN 1528-7483.

Yamada, A.; Chung, S. C. & Hinokuma K. (2001) Optimized LiFePO$_4$ for Lithium Battery Cathodes. *J. Electrochem. Soc.*, Vol. 148, pp. A224-A229, ISSN 0013-4651.

Yang, S. ; Zavalij, P.Y. & Whittingham, M. S. (2001) Hydrothermal Synthesis of Lithium Iron Phosphate Cathodes. *Electrochem. Commun.*, Vol. 3, pp. 505-508, ISSN 1388-2481.

Yang, M-R.; Ke, W-H. & Wu, S-H. (2005) Preparation of LiFePO$_4$ powders by co-precipitation *J. Power Sources*, Vol. 146, pp. 539-543, ISSN 0378-7753.

Yang, H.; Wu, X-L.; Cao, M-H. & Guo, Y-G. (2009) Solvothermal Synthesis of LiFePO$_4$ Hierarchically Dumbbell-Like Microstructures by Nanoplate Self-Assembly and Their Application as a Cathode Material in Lithium-Ion Batteries. *J. Phys. Chem. C*, Vol. 113, pp. 3345-3351, ISSN 1932-7447.

Yang, S.; Zhou, X.; Zhang, J. & Liu, Z. (2010) Morphology-controlled solvothermal synthesis of LiFePO$_4$ as cathode material for lithium-ion batteries. *J. Mater. Chem.*, Vol. 20, pp. 8086-8091, ISSN 0959-9428.

Zhang, S.S.; Allen, J.L.; Xu, K. & Jow, T.R. (2005) Optimization of reaction condition for solid-state synthesis of LiFePO$_4$-C composite cathodes *J. Power Sources*, Vol. 147, pp. 234-240, ISSN 0378-7753.

Zhou, G.; Lü, M.; Yang, Z.; Tian, F.; Zhou, Y. & Zhang, A. (2007) Fabrication of Novel Palladium Microstructures through Self-Assembly. *Cryst. Growth Des.*, Vol. 7, pp. 187-190, ISSN 1528-7483.

Zhu, S.; Zhou, H.; Miyoshi, T.; Hibino, M.; Honma, I. & Ichihara, M. (2004) Self-Assembly of the Mesoporous Electrode Material Li$_3$Fe$_2$(PO$_4$)$_3$ Using a Cationic Surfactant as the Template. *Adv. Mater.*, Vol. 16, pp. 2012-2017, ISSN 1521-4095.

Lithium Ion Batteries - New Developments

Edited by Dr. Ilias Belharouak

ISBN 978-953-51-0077-5

Hard cover, 226 pages

Publisher InTech

Published online 24, February, 2012

Published in print edition February, 2012

The eight chapters in this book cover topics on advanced anode and cathode materials, materials design, materials screening, electrode architectures, diagnostics and materials characterization, and electrode/electrolyte interface characterization for lithium batteries. All these topics were carefully chosen to reflect the most recent advances in the science and technology of rechargeable Li-ion batteries, to provide wide readership with a platform of subjects that will help in the understanding of current technologies, and to shed light on areas of deficiency and to energize prospects for future advances.

How to reference

In order to correctly reference this scholarly work, feel free to copy and paste the following:

Verónica Palomares and Teófilo Rojo (2012). Synthesis Processes for Li-Ion Battery Electrodes – From Solid State Reaction to Solvothermal Self-Assembly Methods, Lithium Ion Batteries - New Developments, Dr. Ilias Belharouak (Ed.), ISBN: 978-953-51-0077-5, InTech, Available from: http://www.intechopen.com/books/lithium-ion-batteries-new-developments/synthesis-processes-for-li-ion-battery-electrodes-from-solid-state-reaction-to-solvothermal-self-ass

INTECH
open science | open minds